

Soil carbon response to warming is dependent on microbial physiology

Steven D. Allison
Matthew D. Wallenstein
Mark A. Bradford

Supplementary Methods

Enzyme-driven model: structure, initialisation, and simulations

Model structure

Our enzyme model is based on the conceptual framework developed by Schimel and Weintraub¹. To this framework (Fig. 1a) we added temperature sensitivity of degradation processes, following established theory relating to soil respiration and biochemical responses to warming^{2,3}. The model starts by setting the soil organic carbon (SOC), dissolved organic carbon (DOC), microbial biomass, and enzyme pools to their initial values. Microbial biomass changes by the amount of DOC assimilated, times the carbon use (or microbial growth) efficiency, minus biomass death and enzyme production:

$$\frac{dMIC}{dt} = ASSIM * CUE - DEATH - EPROD \quad (1)$$

where assimilation is a Michaelis-Menten function scaled to the size of the microbial biomass pool:

$$ASSIM = Vmax_{uptake} * MIC * \frac{DOC}{Km_{uptake} + DOC} \quad (2)$$

We assume that the cell surface area available for uptake will be directly proportional to the number of cells. Microbes may not assimilate more DOC than is available in the DOC pool. Microbial biomass death is modeled as a first-order process with a rate constant r_{death} :

$$DEATH = r_{death} * MIC \quad (3)$$

Enzyme production is modelled as a constant fraction ($r_{EnzProd}$) of microbial biomass:

$$EPROD = r_{EnzProd} * MIC \quad (4)$$

During uptake, the $Vmax$, Km , and carbon use efficiency (CUE) parameters are temperature sensitive. The model calculates a temperature-specific $Vmax$ using the Arrhenius equation, where $Vmax_{uptake_0}$ is the pre-exponential coefficient, gas_{const} is the ideal gas constant, and Ea is the activation energy, or the amount of energy required to convert substrate into product:

$$Vmax_{uptake} = Vmax_{uptake_0} * \exp\left(-\frac{Ea_{uptake}}{gas_{const} * (temp + 273)}\right) \quad (5)$$

SOC with higher Ea reacts more slowly, but the temperature sensitivity of the reaction is greater². Km values are calculated as a linear function of temperature between 0 and 50°C:

$$Km_{uptake} = Km_{uptake_{slope}} * temp + Km_{uptake_0} \quad (6)$$

The CUE is also a linear function of temperature:

$$CUE = CUE_{slope} * temp + CUE_0 \quad (7)$$

CO₂ production is the fraction of DOC assimilated by microbes that is not allocated to biomass production:

$$CO_2 = ASSIM * (1 - CUE) \quad (8)$$

The enzyme pool increases with enzyme production and decreases with enzyme turnover:

$$\frac{dEnz}{dt} = EPROD - ELOSS \quad (9)$$

where enzyme turnover is modelled as a first-order process with a rate constant $r_{EnzLoss}$:

$$ELOSS = r_{EnzLoss} * Enz \quad (10)$$

The SOC pool increases with external inputs and a fraction of dead microbial biomass ($MICtoSOC$) and decreases due to decomposition losses:

$$\frac{dSOC}{dt} = inputSOC + DEATH * MICtoSOC - DECOMP \quad (11)$$

where decomposition of SOC is catalysed according to Michaelis-Menten kinetics by the enzyme pool:

$$DECOMP = Vmax * Enz * \frac{SOC}{Km + SOC} \quad (12)$$

The amount of SOC decomposed may not exceed the total SOC pool. The temperature sensitivity of decomposition is modelled in the same way as uptake, with temperature dependency built into the extracellular enzyme parameters $Vmax$ and Km :

$$Vmax = Vmax_0 * \exp\left(-\frac{Ea}{gas_{const} * (temp + 273)}\right) \quad (13)$$

$$Km = Km_{slope} * temp + Km_0 \quad (14)$$

The DOC pool receives external inputs, the remaining fraction of dead microbial biomass, the decomposition flux, and dead enzymes, while assimilation of DOC by microbial biomass is subtracted:

$$\frac{dDOC}{dt} = inputDOC + DEATH * (1 - MICtoSOC) + DECOMP + ELOSS - ASSIM \quad (15)$$

Model initialisation

After running the model with the spin-up parameters in Supplementary Table 2, pool sizes of SOC, DOC, microbial biomass, and extracellular enzymes equilibrated at reasonable proportions. For example, microbial biomass represented approximately 2% of SOC, consistent with empirical studies⁴. These equilibrium pool sizes were used as default initial values (Supplementary Table 2) in subsequent model simulations.

Model simulations and parameter justification

We simulated warming by increasing temperature from 20°C to 25°C and varied the temperature sensitivity of CUE in our analyses between zero and $-0.016 \text{ }^{\circ}\text{C}^{-1}$. We also conducted runs with constant CUE by fixing this parameter at 0.31, its value at 20°C. These values are reasonable given that microbial CUE varies widely across ecosystems, from 0.01 to 0.85⁵. Physiological studies with bacteria suggest that CUE (a.k.a. growth efficiency or growth yield) should decline with increasing temperature because maintenance respiration increases more steeply than biomass production^{6–8}. The increase in respiration is thought to be driven by more rapid protein turnover and increased energy requirements to maintain ion gradients across the cell membrane at higher temperatures^{6–8}. However, the direct influence of temperature on CUE in more complex communities remains uncertain.

In soil systems, there are relatively few measurements of CUE temperature response, but all show a consistent pattern of declining CUE with increased temperature. Following addition of rice straw to soil microcosms, Devêvre and Horwath⁹ found a decline in CUE of $\sim 0.012 \text{ }^{\circ}\text{C}^{-1}$ across a temperature range of 5°C to 25°C. Van Ginkel et al.¹⁰ observed a decline in CUE of ^{14}C -labeled grass roots from 0.444 to 0.347 when the incubation temperature increased from 14°C to 16°C. This corresponds to a CUE temperature dependence of $-0.049 \text{ }^{\circ}\text{C}^{-1}$, although the measurement was replicated only once. Although they did not calculate CUE, Pietikäinen et al.¹¹ found that soil bacterial and fungal respiration increased exponentially up to 45°C while growth increased linearly and then declined above 25°C, suggesting a sharp decline in CUE at higher temperatures. Finally, Steinweg et al.¹² measured a CUE temperature dependence of $-0.009 \text{ }^{\circ}\text{C}^{-1}$ across a temperature range of 15°C to 25°C using cellobiose as a substrate.

Bacterial growth efficiency (equivalent to CUE) has been measured much more frequently in marine and freshwater systems, but there has been substantial controversy over its temperature response. A 1998 literature review by del Giorgio et al.¹³ did not find a temperature response, but in another global analysis of ocean systems, Rivkin and Legendre¹⁴ found a negative relationship of the form $0.374 - 0.0104 \cdot T$. López-Urrutia and Morán¹⁵ later argued that the negative relationship was due to a confounding effect of resource availability rather than temperature; at low latitudes in the ocean, nutrient availabilities are often low and may constrain bacterial growth efficiency. However, a recent study in estuarine systems found that bacterial growth efficiency declined by $0.014 \text{ }^{\circ}\text{C}^{-1}$, and argued that both temperature and nutrient availability controlled the relationship¹⁶.

One difference between the research in aquatic versus soil systems is that the former has focused on bacterial CUE and the latter on microbial (i.e. bacteria + fungal) CUE. We do not know whether fungal CUE might respond differently to temperature than bacterial CUE, and

hence explain why the relationship between temperature and CUE is consistently negative in soils but more uncertain in aquatic systems. Yet given the few measures of microbial CUE in soils, and the debate about temperature sensitivity of bacterial CUE in aquatic systems, we felt it important to model both declining and constant CUE with increasing temperature.

We simulated microbial acclimation and altered C inputs in several ways. To represent acclimation of CUE, we reduced its temperature sensitivity by 50% under warming (resulting in a value of 0.27 instead of 0.23). Acclimation of extracellular and uptake enzyme kinetics was accomplished by making V_{max} half as sensitive and K_m 50% more sensitive to a 5°C increase in temperature³. This representation of acclimation reduces the sensitivity of total enzymatic activity to a change in temperature, as assumed in literature definitions and following expected biochemical trade-offs^{17,18}. Runs with altered C inputs involved 20% reductions or increases in both the DOC and SOC inputs. Since very few (if any) studies have directly measured the temperature sensitivities of plant inputs or enzyme kinetic parameters in soil, our parameter manipulations are necessarily arbitrary. However, varying these parameters is useful for identifying potentially important biological controls on SOC turnover and stimulating future empirical work to fill gaps in knowledge. These parameter manipulations were ultimately chosen because they represent alternate explanations for the ephemeral increase of soil respiration with elevated temperature^{17,19-24}.

Enzyme-driven model: sensitivity analysis

We conducted a model sensitivity analysis by varying parameters over two orders of magnitude, or a broad range of their possible values. We used the latter approach for the slope and intercept of the CUE temperature function because these parameters are unlikely to vary over orders of magnitude. We assessed the sensitivities of the model pool sizes and CO₂ fluxes in the analysis. Sensitivity is expressed as:

$$\frac{|\log_{10}|High\ output| - \log_{10}|Low\ output||}{|\log_{10}|High\ parameter| - \log_{10}|Low\ parameter||} \quad (16)$$

Order of magnitude changes in several of the parameters resulted in disproportionate changes in some of the output variables (Supplementary Table 1). SOC pools were most sensitive to changes in the E_a for SOC degradation. This sensitivity is logical because E_a appears in the exponent of the Arrhenius relationship that determines SOC decay rates. SOC, microbial biomass, and enzyme pools were all highly sensitive to the intercept of the microbial CUE function. They were also sensitive to the slope, but to a lesser extent. SOC was also moderately sensitive to enzyme and microbial biomass turnover rates, as well as enzyme production rates. Sensitivities for most other parameter-response combinations were <1, meaning that an order of magnitude change in the parameter resulted in less than an order of magnitude change in the response variable.

Supplementary Discussion

Enzyme-driven model: behaviours

Following established biochemical theory^{2,3}, predictions from models based on empirical responses of soil respiration and SOC to warming^{20,21}, and empirical observations^{17,25}, we would expect our model to exhibit a number of different behaviours. We first established that ‘apparent’ temperature sensitivity (Q_{10}) of respiration declined with increasing temperature and increased if we increased the availability of DOC substrate². We also verified that the model recreates the positive, short-term response of soil respiration to warming due to the temperature sensitivity of enzymatic and uptake processes. Next, we determined that soil microbes are C-limited¹ under control scenarios by demonstrating that higher input rates of DOC increased respiration in the short-term (to an asymptote). Next, for the seven scenarios that qualitatively recreated observed patterns of soil respiration and microbial biomass in response to experimental warming in the field^{17,19,25} (Table 1), we established that the following behaviours were realised. First, cessation of warming (i.e. return to the control temperature of 20°C) resulted in an immediate drop in respiration values below the control scenario^{17,21}. Second, addition of unlimited substrate (i.e. DOC) did not obscure this observation (due to the lower microbial biomass)¹⁷. Third, if respiration rates for the test of the second behaviour are divided by the microbial biomass, the calculated mass specific respiration rates are markedly lower than control values only for scenarios where V_{max} and K_m have been ‘acclimated’^{3,17}. Overall then we were able to demonstrate that the model structure elicited behaviours consistent with current biochemical and soil biogeochemical theory^{1-3,20,21}, and that at least seven scenarios (see Table 1) generated predictions qualitatively consistent with empirical observations under field warming^{17,19,25} but with markedly different implications for the magnitude of soil C loss.

Conventional model: structure and predictions

We constructed a second model with a structure representative of conventional box models of SOC dynamics^{20,26}. This model (Fig. 1b) included SOC, DOC, and microbial biomass C pools as well as temperature sensitivity of decomposition, but omitted the extracellular enzyme pool. The decomposition rate of each pool was represented as a first-order process with the decay constant k increasing exponentially with temperature according to the Arrhenius relationship:

$$k_{DOC} = k_{DOC_0} * \exp\left(-\frac{Ea_{DOC}}{gas_{const} * (temp + 273)}\right) \quad (17)$$

$$k_{SOC} = k_{SOC_0} * \exp\left(-\frac{Ea_{SOC}}{gas_{const} * (temp + 273)}\right) \quad (18)$$

$$k_{MIC} = k_{MIC_0} * \exp\left(-\frac{Ea_{MIC}}{gas_{const} * (temp + 273)}\right) \quad (19)$$

where k_0 is the pre-exponential coefficient and Ea is the activation energy. DOC, SOC, and MIC refer to the different C pools. Decomposition of each pool was represented as:

$$SOC_{DECOMP} = kSOC * SOC \quad (20)$$

$$DOC_{DECOMP} = kDOC * DOC \quad (21)$$

$$DEATH = kMIC * MIC \quad (22)$$

The change in the SOC pool is proportional to external inputs, transfers from the other pools, and losses due to first-order decomposition:

$$\frac{dSOC}{dt} = inputSOC + DOctoSOC * DOC_{DECOMP} + MICtoOC * MICtoSOC * DEATH - SOC_{DECOMP} \quad (23)$$

where *DOctoSOC* is the transfer coefficient from the DOC to the SOC pool, *MICtoOC* is the transfer coefficient from the MIC to the DOC and SOC pools, and *MICtoSOC* is the partition coefficient for dead microbial biomass between the SOC and DOC pools. Transfer coefficients can range from 0.0 to 1.0, with lower values indicating a larger fraction of C respired as CO₂. The change in the DOC pool is represented similarly, but includes a loss due to microbial uptake:

$$\frac{dDOC}{dt} = inputDOC + SOCtoDOC * SOC_{DECOMP} + MICtoOC * (1 - MICtoSOC) * DEATH - f_{uptake} * DOC - DOC_{DECOMP} \quad (24)$$

The change in the microbial biomass pool is simply the difference between uptake and turnover, where *f_{uptake}* represents the fraction h⁻¹ of the DOC pool taken up by microbial biomass:

$$\frac{dMIC}{dt} = f_{uptake} * DOC - DEATH \quad (25)$$

Thus we assume that the availability of DOC controls microbial growth rates.

We ran the model with the spinup and default parameters listed in Supplementary Table 3. These parameters were chosen to generate conditions similar to the enzyme-based model. We set the *Ea* for SOC to the same value of 47 kJ mol⁻¹ and assigned lower values of 40 kJ mol⁻¹ to the DOC and microbial biomass pools. We then adjusted the pre-exponential coefficients so that equilibrium pool sizes were similar to our other model. We assumed that all transfers between pools were 20% efficient, but reduced this value to 10% to simulate changes in microbial CUE.

After running the conventional model to equilibrium, warming by 5°C resulted in large losses of SOC (Fig. 3). There were also comparable declines in DOC and microbial biomass pools, indicative of substrate depletion. In contrast to the enzyme-based model, reductions in microbial CUE further increased C losses under warming (Fig. 3). Although microbial biomass declined to a similar extent in the conventional model, there was no direct impact on the SOC pool. All loss rates were controlled solely by the first order decay constants, which increased exponentially with warming. Our comparison demonstrates that microbial biomass and enzymes must directly catalyse SOC decomposition to account for warming effects on microbial physiology. Without this model structure, there is no mechanism by which changes in microbial CUE or acclimation within the microbial community can affect SOC pools.

Supplementary Tables**Supplementary Table 1. Sensitivity values for enzyme model parameters.**

Parameter	Sensitivity				
	SOC	DOC	Biomass	Enzyme	CO ₂
<i>inputSOC</i>	0.33	0.50	0.50	0.50	0.50
<i>inputDOC</i>	0.33	0.50	0.50	0.50	0.50
<i>r_{death}</i>	1.47	0.24	1.05	1.05	0.10
<i>r_{EnzProd}</i>	1.47	0.10	0.05	1.05	0.10
<i>r_{EnzLoss}</i>	1.50	0.10	0.10	1.10	0.10
<i>MICtoSOC</i>	0.33	0	0	0	0
<i>CUE₀</i>	5.18	1.66	5.44	5.44	0.58
<i>CUE_{slope}</i>	1.25	0.46	1.49	1.49	0
<i>Vmax₀</i>	1.50	0.10	0.10	0.10	0.10
<i>Vmax_{uptake0}</i>	0	0.26	0	0	0
<i>Km₀</i>	0.77	0	0	0	0
<i>Km_{uptake0}</i>	0	0.04	0	0	0
<i>Km_{slope}</i>	0.23	0	0	0	0
<i>Km_{uptake_{slope}}</i>	0	0.17	0	0	0
<i>Ea</i>	23.63	0	0	0	0
<i>Ea_{uptake}</i>	0	0	0	0	0

Supplementary Table 2. Spinup and default parameter values for enzyme model runs.

Parameter	Units	Spinup	Defaults
<i>endTime</i>	h	24000000	262800
<i>interval</i>	h	240000	8760
<i>temp</i>	0 to 50 °C	20	20
<i>initSOC</i>	mg cm ⁻³	100	111.876
<i>initDOC</i>	mg cm ⁻³	0.5	0.00144928
<i>initMIC</i>	mg cm ⁻³	0.5	2.19159
<i>initEnz</i>	mg cm ⁻³	0.01	0.0109579
<i>inputSOC</i>	mg cm ⁻³ h ⁻¹	0.0005	0.0005
<i>inputDOC</i>	mg cm ⁻³ h ⁻¹	0.0005	0.0005
<i>r_{death}</i>	h ⁻¹	0.0002	0.0002
<i>r_{EnzProd}</i>	h ⁻¹	0.000005	0.000005
<i>r_{EnzLoss}</i>	h ⁻¹	0.001	0.001
<i>MICtoSOC</i>	mg mg ⁻¹	0.5	0.5
<i>CUE₀</i>	mg mg ⁻¹	0.63	0.63
<i>CUE_{slope}</i>	degree ⁻¹	-0.016	-0.016
<i>Vmax₀</i>	mg SOM cm ⁻³ (mg Enz cm ⁻³) ⁻¹ h ⁻¹	100000000	100000000
<i>Vmax_{uptake₀}</i>	mg DOC cm ⁻³ (mg biomass cm ⁻³) ⁻¹ h ⁻¹	100000000	100000000
<i>Km₀</i>	mg cm ⁻³	500	500
<i>Km_{uptake₀}</i>	mg cm ⁻³	0.1	0.1
<i>Km_{slope}</i>	mg cm ⁻³ degree ⁻¹	5	5
<i>Km_{uptake_{slope}}</i>	mg cm ⁻³ degree ⁻¹	0.01	0.01
<i>Ea</i>	kJ mol ⁻¹	47	47
<i>Ea_{uptake}</i>	kJ mol ⁻¹	47	47
<i>gas_{const}</i>	kJ mol ⁻¹ degree ⁻¹	0.008314	0.008314

Supplementary Table 3. Spinup and default parameter values for conventional model runs.

Parameter	Units	Spinup	Defaults
<i>endTime</i>	h	10000000	262800
<i>interval</i>	h	100000	8760
<i>temp</i>	0 to 50 °C	20	20
<i>initSOC</i>	mg cm ⁻³	100	111.121
<i>initDOC</i>	mg cm ⁻³	0.5	0.521927
<i>initMIC</i>	mg cm ⁻³	0.5	2.20661
<i>inputSOC</i>	mg cm ⁻³ h ⁻¹	0.0005	0.0005
<i>inputDOC</i>	mg cm ⁻³ h ⁻¹	0.0005	0.0005
<i>f_{uptake}</i>	h ⁻¹	0.0005	0.0005
<i>gas_{const}</i>	kJ mol ⁻¹ K ⁻¹	0.008314	0.008314
<i>kDOC₀</i>	h ⁻¹	10000	10000
<i>KSOC₀</i>	h ⁻¹	1300	1300
<i>kMIC₀</i>	h ⁻¹	1600	1600
<i>Ea_{DOC}</i>	kJ mol ⁻¹	40	40
<i>Ea_{SOC}</i>	kJ mol ⁻¹	47	47
<i>Ea_{MIC}</i>	kJ mol ⁻¹	40	40
<i>DOctoSOC</i>	mg mg ⁻¹	0.2	0.2
<i>SOCtoDOC</i>	mg mg ⁻¹	0.2	0.2
<i>MICtoOC</i>	mg mg ⁻¹	0.2	0.2
<i>MICtoSOC</i>	mg mg ⁻¹	0.5	0.5

Supplementary Notes

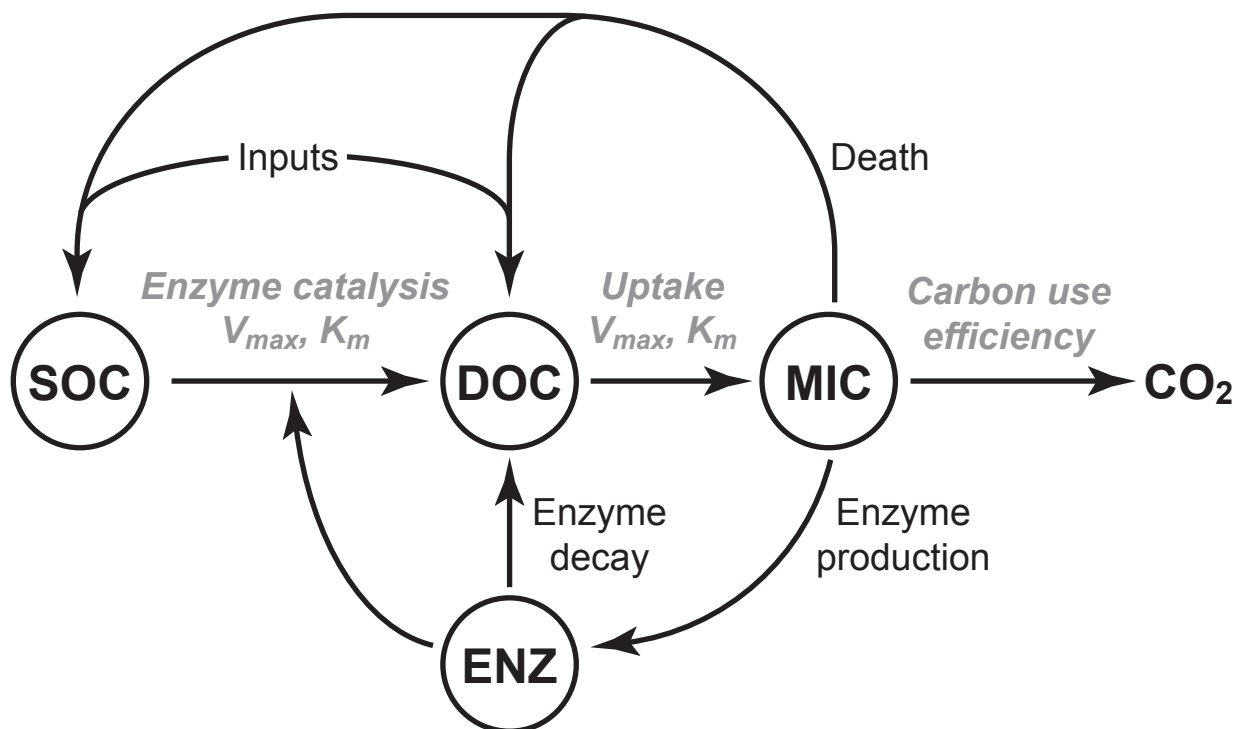
1. Schimel, J. P. & Weintraub, M. N. The implications of exoenzyme activity on microbial carbon and nitrogen limitation in soil: a theoretical model. *Soil Biol. Biochem.* **35**, 549-563 (2003).
2. Davidson, E. A. & Janssens, I. A. Temperature sensitivity of soil carbon decomposition and feedbacks to climate change. *Nature* **440**, 165-173 (2006).
3. Hochachka, P. W. & Somero, G. N. *Biochemical Adaptation: Mechanism and Process in Physiological Evolution* (Oxford University Press, Oxford, 2002).
4. Fierer, N., Strickland, M. S., Liptzin, D., Bradford, M. A. & Cleveland, C. C. Global patterns in belowground communities. *Ecol. Lett.* **12**, 1238-1249 (2009).
5. Six, J., Frey, S. D., Thiet, R. K. & Batten, K. M. Bacterial and fungal contributions to carbon sequestration in agroecosystems. *Soil Sci. Soc. Am. J.* **70**, 555-569 (2006).
6. Hall, E. K. & Cotner, J. B. Interactive effect of temperature and resources on carbon cycling by freshwater bacterioplankton communities. *Aquat. Microb. Ecol.* **49**, 35-45 (2007).
7. Farmer, I. S. & Jones, C. W. The effect of temperature on the molar growth yield and maintenance requirement of *Escherichia coli* W during aerobic growth in continuous culture. *FEBS Lett.* **67**, 359-363 (1976).
8. Mainzer, S. E. & Hempfling, W. P. Effects of growth temperature on yield and maintenance during glucose-limited continuous culture of *Escherichia coli*. *J. Bacteriol.* **126**, 251-256 (1976).
9. Devêvre, O. C. & Horwath, W. R. Decomposition of rice straw and microbial carbon use efficiency under different soil temperatures and moistures. *Soil Biol. Biochem.* **32**, 1773-1785 (2000).
10. van Ginkel, J. H., Gorissen, A. & Polci, D. Elevated atmospheric carbon dioxide concentration: effects of increased carbon input in a *Lolium perenne* soil on microorganisms and decomposition. *Soil Biol. Biochem.* **32**, 449-456 (2000).
11. Pietikäinen, J., Pettersson, M. & Bååth, E. Comparison of temperature effects on soil respiration and bacterial and fungal growth rates. *FEMS Microbiol. Ecol.* **52**, 49-58 (2005).
12. Steinweg, J. M., Plante, A. F., Conant, R. T., Paul, E. A. & Tanaka, D. L. Patterns of substrate utilization during long-term incubations at different temperatures. *Soil Biol. Biochem.* **40**, 2722-2728 (2008).
13. del Giorgio, P. A. & Cole, J. J. Bacterial growth efficiency in natural aquatic ecosystems. *Annu. Rev. Ecol. Syst.* **29**, 503-541 (1998).
14. Rivkin, R. B. & Legendre, L. Biogenic carbon cycling in the upper ocean: Effects of microbial respiration. *Science* **291**, 2398-2400 (2001).
15. López-Urrutia, Á. & Morán, X. A. G. Resource limitation of bacterial production distorts the temperature dependence of oceanic carbon cycling. *Ecology* **88**, 817-822 (2007).
16. Apple, J. K., Del Giorgio, P. A. & Kemp, W. M. Temperature regulation of bacterial production, respiration, and growth efficiency in a temperate salt-marsh estuary. *Aquat. Microb. Ecol.* **43**, 243-254 (2006).
17. Bradford, M. A. et al. Thermal adaptation of soil microbial respiration to elevated temperature. *Ecol. Lett.* **11**, 1316-1327 (2008).

18. Hartley, I. P., Hopkins, D. W., Garnett, M. H., Sommerkorn, M. & Wookey, P. A. Soil microbial respiration in arctic soil does not acclimate to temperature. *Ecol. Lett.* **11**, 1092-1100 (2008).
19. Melillo, J. M. et al. Soil warming and carbon-cycle feedbacks to the climate system. *Science* **298**, 2173-2176 (2002).
20. Knorr, W., Prentice, I. C., House, J. I. & Holland, E. A. Long-term sensitivity of soil carbon turnover to warming. *Nature* **433**, 298-301 (2005).
21. Kirschbaum, M. U. F. Soil respiration under prolonged soil warming: are rate reductions caused by acclimation or substrate loss? *Glob. Change Biol.* **10**, 1870-1877 (2004).
22. Eliasson, P. E. et al. The response of heterotrophic CO₂ flux to soil warming. *Glob. Change Biol.* **11**, 167-181 (2005).
23. Luo, Y. Q., Wan, S. Q., Hui, D. F. & Wallace, L. L. Acclimatization of soil respiration to warming in a tall grass prairie. *Nature* **413**, 622-625 (2001).
24. Saleska, S. R., Harte, J. N. & Torn, M. S. The effect of experimental ecosystem warming on CO₂ fluxes in a montane meadow. *Glob. Change Biol.* **5**, 125-141 (1999).
25. Frey, S. D., Drijber, R., Smith, H. & Melillo, J. Microbial biomass, functional capacity, and community structure after 12 years of soil warming. *Soil Biol. Biochem.* **40**, 2904-2907 (2008).
26. Parton, W. J., Stewart, J. W. B. & Cole, C. V. Dynamics of C, N, P, and S in grassland soils - a model. *Biogeochemistry* **5**, 109-131 (1988).

Supplementary Information

This file contains details on the structure, equations, parameters, and behavior of the enzyme-based and conventional models. Supplementary Table 1 contains results from a model sensitivity analysis, and Supplementary Tables 2 and 3 contain model parameters. (Adobe .pdf; 69 kb).

(a) Enzyme model



(b) Conventional model

